Physical Chemistry

The nature of the O—O bond in hydroperoxides

K. A. Lysenko, M. Yu. Antipin, and V. N. Khrustalev*

A. N. Nesmeyanov Institute of Organoelement Compounds, Russian Academy of Sciences, 28 ul. Vavilova, 119991 Moscow, Russian Federation. Fax: +7 (095) 135 5085. E-mail: kostya@xrlab.ineos.ac.ru

Quantum-chemical calculations of the H_2O_2 and F_2 molecules using different computational schemes, basis sets, and procedures for the inclusion of electron correlation were performed. High-resolution X-ray diffraction study of the electron density distribution in the crystals of 2,5-dimethyl-2,5-dihydroperoxyhexane and 2,5-dimethyl-2,5-dihydroperoxyhex-3-yne was carried out. Joint analysis of the results obtained showed that the formally covalent O—O and F—F bonds correspond to a specific type of interatomic interaction. This type is intermediate between the shared and closed-shell interactions (the latter are typical of the ionic systems and van der Waals molecules).

Key words: peroxides, electron density distribution, chemical bonding, X-ray diffraction studies, nonempirical quantum-chemical calculations, topological analysis of the electron density distribution, O—O bond.

X-Ray diffraction studies of the electron density distribution, $\rho(\mathbf{r})$, in crystals are among the most widely used experimental methods of analysis of the nature of the chemical bond. Early in the development of this method, analysis of the difference maps, $\Delta\rho(\mathbf{r})$, and, in particular, the deformation electron density (DED) maps was in fact the sole way of investigating the electron density distribution in the region of a chemical bond. The DED calculations include subtraction of the so-called "promolecule" (a superposition of the electron densities of spherically symmetric, noninteracting atoms located at the same positions as those occupied by the atoms in the real molecule or crystal) from the total electron density. Therefore, the DED map shows how the electron density is redistributed upon the formation of a chemical bond between initially noninteracting atoms.

By the early 1980s it was found that most of covalent bonds are characterized by the DED maxima in the interatomic space on the corresponding maps, while ionic or highly polar bonds are characterized by low or even zero DED in the interatomic space and that the DED minima are often observed in such regions.[1—3] This was in good agreement with the traditional opinion, according to which the formation of a covalent bond is a result of electron pair sharing. Such an approach has found a wide use in studies of different types of chemical bonds.[1,2] Moreover, analysis of the experimental DED maps became a nearly usual attribute of high-resolution X-ray diffraction studies of single crystals, which received then particularly wide acceptance. To some extent, this was due to the relative ease of constructing the experimental DED maps, which could be done without performing quantum-chemical calculations.

Published in Russian in *Izvestiya Akademii Nauk. Seriya Khimicheskaya,* No. 9, pp. 1465—1474, September, 2001.

1066-5285/01/5009-1539 $25.00

However, the results of the studies of the O—O bond in hydrogen peroxide[4] and other molecules with single N—O and N—N bonds and with M—M bonds in binuclear complexes[5] soon violated such a promising development of this approach and strongly shaked chemist's faith in the information obtained from the DED analysis. In particular, low-temperature high-resolution X-ray diffraction studies of hydrogen peroxide[4] and 1,2,7,8-tetraaza-4,5,10,11-tetraoxatricyclo[6.4.1.$1^{2,7}$]tetradecane[6] containing single C—O, N—O, and O—O bonds revealed a DED minimum rather than maximum in the region of the homopolar O—O bond.[4,6] In other words, it was found that for real molecules the accumulation of the electron density in the interatomic space is smaller than in the "promolecule". Mention should be made that the depletion of $\rho(\mathbf{r})$ for homopolar bonds was first experimentally found taking the O—O bond as an example and the first theoretical study[7] on the subject concerned the F_2 molecule.

It should be emphasized that such an anomaly for the formally covalent, single bonds was observed only in those cases where the atoms involved in the bonding had more than half-filled valence shells. It is known[3] that in this situation the DED minima observed in the regions of the O—O, F—F, *etc.* bonds are to some extent artifacts associated with the "overresidue" of $\rho(\mathbf{r})$ in the corresponding "promolecules". The models which used either hybridized or "oriented" atoms (see below) as the reference state allowed one to obtain the desired maximum of $\Delta\rho(\mathbf{r})$ in the interatomic space even for the F_2 molecule. Nevertheless, the assumption of a specific type of the interatomic interaction in these molecules can appear to be realistic, especially taking into account the peculiarities of the O—O and F—F bonds (their anomalous lengthening and a decrease in energy as compared to other homopolar bonds formed by the second-row elements, see, *e.g.*, Refs. 8 and 9).

Initially, the O—O and F—F bonds were not placed into a specific group. Their weakening was explained by the Pitzer interatomic repulsion[10,11] or, more recently, by the intraatomic repulsion between the lone electron pairs (LEP).[12] The latter model implies that weakening of a bond is due to the repulsion between the LEP of the atom and the electron density in the interatomic space; in other words, this effect is a characteristic of the atom rather than of the bond.[12]

Calculations of the difference functions $\Delta\rho(\mathbf{r})$ performed using the reference functions that take into account the polarization and orientation of the atom lead to accumulation of the electron density in the regions of O—O and F—F bonds.[13—16] Undoubtedly, the use of such a "specially derived" electron density[13] is more correct, since the interactions, which can lead to particular orientation of the electron density of the atom involved in the formation of a chemical bond, occur even at rather long interatomic distances.[16] In this case, the absence of the DED maxima in the region of the O—O and F—F bonds results from overresidue of the electron density at the midpoint of the bond and is due to partial filling of the valence shell.[3] For instance, ignoring the linear combination of the components of the ground-state ^2P term of the F atom in the F_2 molecule leads to subtraction of a total of 5/3 e instead of 1 e at the midpoint of the F—F bond and to the appearance of a "hole" on the DED maps.[13]

Discussion about the character of the F—F bond in the F_2 molecule and the O—O bond in peroxides was continued after the appearance of the theory of "atoms in molecule" (AM) by R. Bader.[17—20] This theory treats the chemical bond in a molecule based on the results of analysis of the values of the function $\rho(\mathbf{r})$ and its Laplacian, $\nabla^2\rho(\mathbf{r})$, at the critical points (CT) at which the gradient of $\rho(\mathbf{r})$ equals zero.[17] Taking into account the topology of the function $\rho(\mathbf{r})$ at the CT (3, −1)*, the AM theory divides all interatomic interactions into covalent and closed-shell ones (the latter are typical of ionic, strongly polar, and van der Waals bonds).[17,20] Covalent interactions are characterized by negative $\nabla^2\rho(\mathbf{r})$ values and high $\rho(\mathbf{r})$ at the CT (3, −1). In the case of closed-shell interactions, the Laplacian $\nabla^2\rho(\mathbf{r})$ at the corresponding CT is positive while the electron density is low.[17—20] However, positive values of the Laplacian $\nabla^2\rho(\mathbf{r})$ cannot be considered as unambiguous criterion for the closed-shell interaction.

In the framework of the AM theory, the positive value of the local energy density $E(\mathbf{r})$

$$E(\mathbf{r}) = V(\mathbf{r}) + G(\mathbf{r}), \qquad (1)$$

where $G(\mathbf{r})$ and $V(\mathbf{r})$ are the local densities of the kinetic and potential energies, respectively, is the necessary condition for the closed-shell interaction. Taking into account that the Laplacian of $\rho(\mathbf{r})$, $\nabla^2\rho(\mathbf{r})$, appears in the local expression of the virial theorem,[17,19,20]

$$(\hbar^2/4m)\nabla^2\rho(\mathbf{r}) = 2G(\mathbf{r}) + V(\mathbf{r}), \qquad (2)$$

we get:

$$E(\mathbf{r}) = V(\mathbf{r}) + G(\mathbf{r}) = (\hbar^2/4m)\nabla^2\rho(\mathbf{r}) - G(\mathbf{r}). \qquad (3)$$

From expression (3) it follows that the positive value of $\nabla^2\rho(\mathbf{r})$ cannot ensure a positive local energy density, since $E(\mathbf{r})$ can remain negative if the density of the potential energy (by definition, it has a negative value) is higher in absolute value than the density of the kinetic energy. The bonds characterized by a positive Laplacian and a negative $E(\mathbf{r})$ at the CT (3, −1) correspond to the intermediate type of interatomic interactions.[17—20] The term "intermediate" seems to be due to the fact that in this case the topology of the function $\rho(\mathbf{r})$ at the

* The presence, in the interatomic space, of the critical points (3, −1), which are characterized by non-zero eigenvalues of the Hesse matrix and at which the algebraic sum of their signs equals −1, is a necessary and sufficient criterion for the formation of a chemical bond.[17,20]

CT (3, −1) has the same visual pattern as in the case of the closed-shell interactions, while the ratio of the contributions of the densities of the kinetic and potential energies corresponds to the covalent interaction. The character of the interatomic interaction can also be assessed from the ratio of the eigenvalues of the Hesse matrix, ($|\lambda_1/\lambda_3|$), and the $G(\mathbf{r})/\rho(\mathbf{r})$ value, which for the closed-shell interactions must be smaller and larger than unity, respectively.[15—18]

It should be noted that classification of chemical bonds based on analysis of the topology of the electron density distribution becomes more and more popular. Applications and advantages of this approach in the case of the function $\rho(\mathbf{r})$ obtained from X-ray diffraction data have been the subject of a recent discussion.[21—23] In this connection, it is of interest to perform a comparative study of the "anomalous" nature of the O—O bond in hydrogen peroxide and other hydroperoxide molecules and that of the F—F bond in the F_2 molecule. In this work, we present the results of a theoretical study of the F_2 and H_2O_2 molecules carried out using modern quantum-chemical methods and a high-resolution, low-temperature X-ray diffraction study of the crystals of 2,5-dimethyl-2,5-dihydroperoxyhexane (**1**) and 2,5-dimethyl-2,5-dihydroperoxyhex-3-yne (**2**).

Results and Discussion

The pioneering HF/6-31G* study[18] of the topology of $\rho(\mathbf{r})$ in the F_2 molecule led to the following characteristics at the CT (3, −1): $\rho(\mathbf{r})$ = 2.335 e Å^{-3}, $\nabla^2\rho(\mathbf{r})$ = 2.908 e Å^{-5}, and $E(\mathbf{r})$ = −0.302 au, which points to the intermediate type of the interatomic interaction. One could also expect a similar picture for the H_2O_2 molecule; however, calculations performed in the same study[18] gave a negative value of −9.509 e Å^{-5} for the Laplacian $\nabla^2\rho(\mathbf{r})$ at the CT (3, −1) in the region of the O—O bond. Based on this result and in contrast to the F—F bond in the F_2 molecule, the O—O interaction was assigned to the covalent type.

Notwithstanding the fact that the Hartree—Fock calculations of both molecules, H_2O_2 and F_2, did not reproduce their experimental geometries, numerous more recent studies on the character of the chemical bond were performed only for the latter molecule.[24,25] It was assumed that the inclusion of electron correlation in the F_2 molecule can affect the character of the F—F interaction (the sign of $\nabla^2\rho(\mathbf{r})$ at the CT (3, −1)); however, the application of different procedures (see, *e.g.*, Ref. 26) did not change the character of the results obtained. The sole exception are the results of a recent study,[25] according to which the type of the interatomic interaction in the F_2 molecule, determined in the framework of the AM theory, changes if calculations are carried out in the 6-311+G(3df) basis set augmented with polarization d- and f-functions. This conclusion was drawn based on the change in the sign of $\nabla^2\rho(\mathbf{r})$ at the CT (3, −1) (−1.084 e Å^{-5}).

Unfortunately, no topological characteristics of $\rho(\mathbf{r})$ in the F_2 molecule, obtained with inclusion of electron correlation, were reported in the study cited.[25] This precludes correct estimation of the effect of polarization f-functions and, hence, correctness of the results obtained. Therefore, in this work we report the geometric parameters of and the characteristics of the electron density distributions in the H_2O_2 and F_2 molecules calculated using different basis sets and approximations.

Geometry and topology of ρ(r) in the F_2 molecule

To obtain a correct estimation of the effect of the basis sets and computational methods employed on the topology of $\rho(\mathbf{r})$, we performed a comparative topological analysis of the function $\rho(\mathbf{r})$ for the F_2 molecule calculated in the framework of different approximations. These were the Hartree—Fock (HF) approximation, density functional theory (DFT) with the B3LYP functional, and calculations with inclusion of correlation corrections at the fourth-order Møller—Plesset level of perturbation theory (MP4) and by the configuration interaction method (QCISD). The 6-311G[27] basis set augmented with polarization 3d- and 3df-functions was used. All calculations were carried out with the G94W program package.[28] The results obtained are listed in Table 1.

Table 1. The F—F bond length (R) and topological characteristics of the electron density distribution at the CT (3, −1) in the F_2 molecule calculated by different methods

Method	R /Å	$\rho(\mathbf{r})$ /e Å^{-3}	$\nabla^2\rho(\mathbf{r})$ /e Å^{-5}	$G(\mathbf{r})$	$V(\mathbf{r})$	$E(\mathbf{r})$	$G(\mathbf{r})/\rho(\mathbf{r})$	$\lvert\lambda_1/\lambda_3\rvert$
				au				
HF/6-311+G(3d)	1.3288	2.436	5.805	0.388	−0.617	−0.279	1.07	0.44
HF/6-311+G(3df)	1.3246	2.591	0.713	0.361	−0.714	−0.353	0.94	0.49
B3LYP/6-311+G(3d)	1.4011	1.882	13.085	0.279	−0.421	−0.142	1.00	0.36
B3LYP/6-311+G(3df)	1.3947	1.997	10.555	0.293	−0.477	−0.183	0.98	0.39
QCISD/6-311+G(3d)	1.4095	1.802	14.917	0.295	−0.434	−0.139	1.10	0.31
QCISD/6-311+G(3df)	1.3919	2.000	11.688	0.329	−0.526	−0.202	1.11	0.38
MP4(full,SDQ)/6-311+G(3d)	1.4121	1.788	15.037	0.292	−0.428	−0.136	1.10	0.34
MP4(full,SDQ)/6-311+G(3df)	1.3942	1.991	11.856	0.321	−0.519	−0.199	1.08	0.38
Experiment	1.4165							

As can be seen from the data presented in Table 1, calculations without inclusion of electron correlation lead to substantial underestimation of the F—F bond length (down to 1.3246 Å), whereas in the MP4(SDQ) approximation this parameter is close to the experimental value (1.4165 Å). Augmentation of the basis set with polarization f-functions leads to systematic shortening of the interatomic distance irrespective of the approximation used.

In is known that analysis of the topology of the electron density distribution by the HF/6-311G+(3df) method leads to abnormally small value of the Laplacian of $\rho(\mathbf{r})$ at the CT (3, −1) in the F_2 molecule, whereas the inclusion of electron correlation favors an increase in the value of $\nabla^2\rho(\mathbf{r})$.[29] We found that in all our calculations augmentation of the basis set with polarization f-functions leads to an insignificant decrease in the $\nabla^2\rho(\mathbf{r})$ value and to an increase in $\rho(\mathbf{r})$ at the CT (3, −1) and that the Laplacian has a positive value irrespective of the type of the procedure for inclusion of electron correlation. In spite of substantial increase in $\nabla^2\rho(\mathbf{r})$ in the case of more correct reproduction of the molecular geometry, the local density energy $E(\mathbf{r})$ remains negative. This is typical of covalent bonds and analogous to the results of HF calculations. Thus, our results show that the F—F bond corresponds to the intermediate type of interatomic interaction.

Geometry and topology of ρ(r) in the H_2O_2 molecule

Unlike the F_2 molecule, no detailed studies of the character of the O—O bond in hydrogen peroxide molecule were carried out. We performed the topological analysis of the electron density distribution in the H_2O_2 molecule based on the results of quantum-chemical calculations.

As in the case of the F_2 molecule, correct reproduction of the experimental geometry of the H_2O_2 molecule requires the inclusion of electron correlation and the use of extended basis sets.[30,31] The lack of reliable information on the molecular geometry of H_2O_2 in the gas phase[31,32] additionally complicates the search for the best basis set and computational method. Currently, the parameters obtained[32] using the microwave and IR spectroscopy data[33] and with consideration of torsional motion of the molecule[34] seem to be the most reliable. The gas-phase geometric parameters of the H_2O_2 molecule in the ground vibrational state are as follows: the O—O and O—H bond lengths are 1.452(5) and 0.965(5) Å, respectively, the angle O—O—H is 100(1)°, and the torsion angle H—O—O—H is 112(1)°.[32] These values are in good agreement with the results obtained in one of the most precise quantum-chemical study of the H_2O_2 molecule carried out by the CCSD(T)/cc-pVQZ coupled cluster method (1.452 and 0.963 Å, 99.9°, and 112.5°, respectively).[32] Unfortunately, widely used software has some drawbacks which preclude the use of both the CCSD(T) method and the cc-pVQZ basis set for the topological analysis of $\rho(\mathbf{r})$ in the hydrogen peroxide molecule.*

On the other hand, DFT calculations (especially, with the hybrid functional B3LYP) are characterized not only by the lower computational cost, but also good agreement between the calculated and experimental geometric parameters and by the ability of rather correct reproduction of the topology of the function $\rho(\mathbf{r})$.[26,31] Therefore, in this work we also performed the topological analysis of $\rho(\mathbf{r})$ by the DFT and MP2 methods using (i) the cc-pVDZ and cc-pVTZ basis sets augmented with polarization functions and (ii) the aug-cc-pVDZ and aug-cc-pVTZ basis sets augmented with diffusion functions. To estimate the effect of the basis set on the specific features of the topology of $\rho(\mathbf{r})$, the calculations were also carried out in the 6-311++G basis set augmented with both polarization d- and d,f-functions for O atoms and with polarization p,d-functions for H atoms.

The calculated geometric parameters of H_2O_2 molecule are listed in Table 2. Analysis of the results obtained showed that DFT calculations lead to very good agreement with the experimental results irrespective of the basis set used. Augmentation of the basis sets with polarization functions was found to have little effect on the results of calculations. The use of the 6-311++G basis set led to an insignificant change in the magnitude of the torsion angle. The results of MP2 calculations follow virtually the same pattern. As in the case of the F_2 molecule (see Table 1), augmentation of the 6-311G basis set with polarization f-functions leads to an insignificant shortening of the O—O distance, which was not observed in the calculations with the cc-pVTZ basis set augmented with polarization f-functions for O atoms (see Table 2). The fact that the combination of the DFT approach with the cc-pVTZ basis set provides better agreement with the experimental geometric parameters compared to the results of CCSD(T) calculations[32] should be pointed out.

Topological analysis of the electron density distribution in the H_2O_2 molecule, based on the results of quantum-chemical calculations, showed (see Table 3) that, in contrast to the F_2 molecule, the character of the O—O interaction is strongly dependent on the basis set used. All versions of our calculations revealed the same type of the O—H interatomic bonding, which corresponds to covalent interaction ($\nabla^2\rho(\mathbf{r}) < 0$, $E(\mathbf{r}) < 0$). The value of $\rho(\mathbf{r})$ at the CT (3, −1) in the region of the O—H bond remains virtually unchanged, except for the results of calculations with the cc-pVDZ basis set. In this case, a decrease in the electron density was determined; however, this was found to be consistent with a lengthening of the O—H bond by 0.01 Å. For this bond,

* The G94W program package provides no means for calculations using the electron density obtained by the CCSD(T) method, while the AIMPAC program cannot perform calculations with *g*-functions.

Table 2. Geometric parameters of hydrogen peroxide molecule calculated by different quantum-chemical methods

Method	Bond, *d*/Å		Angle/deg	
	O—O	O—H	OOH	HOOH
B3LYP/cc-pVDZ	1.453	0.973	99.9	117.8
B3LYP/aug-cc-pVDZ	1.451	0.970	100.7	113.2
B3LYP/cc-pVTZ	1.452	0.966	100.4	113.9
B3LYP/aug-cc-pVTZ	1.451	0.967	100.7	113.3
B3LYP/ 6-311++G(3d,3pd)	1.449	0.966	100.8	111.6
B3LYP/ 6-311++G(3df,3pd)	1.446	0.966	100.8	112.5
MP2(full)/cc-pVDZ	1.456	0.970	98.8	118.4
MP2(full)/ aug-cc-pVDZ	1.467	0.971	99.1	113.9
MP2(full)/cc-pVTZ	1.446	0.963	99.4	114.0
MP2(full)/ aug-cc-pVTZ	1.448	0.964	99.7	112.6
MP2(full)/ 6-311++G(3d,3pd)	1.452	0.962	99.7	110.5
MP2(full)/ 6-311++G(3df,3pd)	1.442	0.963	99.9	111.7
CCSD(T)/ cc-pVTZ[32]	1.458	0.964	99.5	113.9
CCSD(T)/ cc-pVQZ[32]	1.452	0.963	99.9	112.5
Experiment[32]	1.452(5)	0.965(5)	100(1)	112(1)

the value of the Laplacian $\nabla^2\rho(\mathbf{r})$ is more sensitive to the basis set; its magnitude increases from −50.42 to −74.35 e Å^{-5} on going from the cc-pVDZ to the 6-311G basis set.

It can be assumed that changes in the $\nabla^2\rho(\mathbf{r})$ values are accompanied by changes in the local energy characteristics (see Eqs. (1)—(3)). Indeed, a change in $\nabla^2\rho(\mathbf{r})$ is first of all determined (see Table 3) by a substantial increase in the density of the potential energy $V(\mathbf{r})$, the magnitude of which increases from −0.656 to −0.902 au (DFT) and from −0.686 to −0.928 au (MP2) on going from the cc-pVDZ to the 6-311++G(3df,3pd) basis set.

We found that the topological characteristics of the O—O bond depend not only on the basis set, but also on the computational method employed. In particular, the results of DFT calculations in the cc-pVDZ, aug-cc-pVDZ, and 6-311++G(3df,3pd) basis sets show that the O—O bond should be considered covalent, since $\nabla^2\rho(\mathbf{r}) < 0$ at the CT (3, −1). On the other hand, both MP2/cc-pVDZ and MP2/6-311++G(3df,3pd) calculations indicate the covalent character of this bond. In other cases, the nature of the O—O bond in the H_2O_2 molecule corresponds to the intermediate type of interatomic interaction. It should be noted that the local density of the potential energy $V(\mathbf{r})$ changes in a rather narrow range on going from one basis set to another, namely, from −0.408 to −0.348 au (B3LYP) and from

Table 3. Topological characteristics of the electron density distribution at the CT (3, −1) in H_2O_2 molecule obtained from quantum-chemical calculations

Method	$\rho(\mathbf{r})$ /e Å^{-3}	$\nabla^2\rho(\mathbf{r})$ /e Å^{-5}	$G(\mathbf{r})$	$V(\mathbf{r})$	$E(\mathbf{r})$	$G(\mathbf{r})/\rho(\mathbf{r})$	$\lvert\lambda_1/\lambda_3\rvert$
			au				
B3LYP/cc-pVDZ	1.854*	−2.169	0.192	−0.407	−0.214	0.70	0.55
	2.355	−50.417	0.066	−0.656	−0.589	0.19	1.23
B3LYP/aug-cc-pVDZ	1.880	−2.579	0.192	−0.411	−0.219	0.69	0.56
	2.437	−51.116	0.065	−0.661	−0.595	0.18	1.18
B3LYP/cc-pVTZ	1.860	3.446	0.192	−0.348	−0.156	0.70	0.46
	2.531	−65.538	0.073	−0.826	−0.753	0.20	1.91
B3LYP/aug-cc-pVTZ	1.860	3.446	0.192	−0.348	−0.156	0.70	0.46
	2.525	−65.769	0.072	−0.826	−0.754	0.20	1.91
B3LYP/6-311++G(3d,3pd)	1.860	1.041	0.190	−0.370	−0.180	0.69	0.49
	2.580	−71.726	0.076	−0.896	−0.821	0.20	2.22
B3LYP/6-311++G(3df,3pd)	1.921	−0.940	0.199	−0.408	−0.209	0.70	0.53
	2.578	−74.349	0.075	−0.902	−0.827	0.20	2.15
MP2(full)/cc-pVDZ	1.806	−0.819	0.205	−0.418	−0.212	0.77	0.53
	2.366	−51.02	0.078	−0.686	−0.607	0.22	1.24
MP2(full)/aug-cc-pVDZ	1.752	0.024	0.198	−0.396	−0.198	0.76	0.51
	2.386	−50.803	0.075	−0.676	−0.602	0.21	1.20
MP2(full)/cc-pVTZ	1.874	3.856	0.214	−0.388	−0.174	0.77	0.45
	2.507	−66.034	0.081	−0.848	−0.766	0.22	1.82
MP2(full)/aug-cc-pVTZ	1.873	3.856	0.213	−0.386	−0.173	0.77	0.45
	2.487	−65.938	0.079	−0.843	−0.763	0.22	1.82
MP2(full)/6-311++G(3d,3pd)	1.822	2.048	0.204	−0.387	−0.183	0.76	0.47
	2.547	−73.168	0.086	−0.930	−0.844	0.23	2.12
MP2(full)/6-311++G(3df,3pd)	1.950	−0.752	0.221	−0.450	−0.228	0.77	0.52
	2.545	−73.197	0.084	−0.928	−0.843	0.22	2.12

* The upper and lower numerical values are given for the O—O and O—H bond, respectively.

−0.450 to −0.396 au (MP2). The local density of the kinetic energy $G(\mathbf{r})$ also changes insignificantly, *viz.*, from 0.190 to 0.199 au (B3LYP) and from 0.198 to 0.221 au (MP2). Nevertheless, this appears to be large enough for the chemist to change the formal interpretation of the character of the O—O interatomic interaction even provided virtually the same molecular geometry.

In the case of the F_2 molecule, the $\nabla^2\rho(\mathbf{r})$ and $E(\mathbf{r})$ values obtained give an unambiguous proof of the intermediate type of interatomic bonding. However, we cannot draw an analogous conclusion based on the results of the topological analysis of the electron density distribution in the H_2O_2 molecule, since the absolute values of $V(\mathbf{r})$ and $G(\mathbf{r})$ are close to each other. Therefore, we studied the distribution and performed the topological analysis of the experimental electron density based on the results of a low-temperature, high-resolution X-ray diffraction study of the crystals of two organic hydroperoxides with electron-donor and electron-acceptor substituents at O atoms, namely, 2,5-dimethyl-2,5-dihydroperoxyhexane (**1**) and 2,5-dimethyl-2,5-dihydroperoxyhex-3-yne (**2**).

Molecular and crystal structures of dihydroperoxides 1 and 2

Our study of dihydroperoxides **1** and **2** showed (Table 4) that in the crystal each molecule occupies a position on a two-fold crystallographic axis passing through the midpoint of the C(2)—C(2′) central bond (see Figs. 1 and 2). In both crystals, the molecules form intermolecular hydrogen bonds of medium length (O...O ≈ 2.73 Å). These bonds are responsible for assembling of the molecules in layers parallel to the **ab** crystallographic plane in the structure of **1** and for the formation of cylindrical helices along the screw axis **c** in the structure of **2**. The principal geometric parameters of molecules **1** and **2** (see Table 5) are in agreement with the expectation. Analysis of the residual electron density peaks in the region of the O(2) atom in the crystal structure of **1** showed that the H atom involved in the formation of the H-bond is statistically disordered over two equally populated positions, H(2OA) and H(2OB).

Analysis of the crystal structures retrieved from the Cambridge Structural Database (CSD, Release 2000) demonstrated that the O—O bond length in organic hydroperoxides varies over a rather wide range (from 1.449 to 1.484 Å, with the average value of 1.463 Å); introduction of electron-donor substituents into the

Table 4. Principal crystallographic parameters and characteristics of the refinement of the crystal structure of compounds **1** and **2**

Parameter	**1**	**2**
Empirical formula	$C_8H_{18}O_4$	$C_8H_{14}O_4$
Molecular weight	178.22	174.19
T/K	153	193
Space group	$C2/c$	$P4_12_12$
Radiation	Mo-Kα (λ = 0.71072 Å)	
Scan type	θ/2θ	
Diffractometer	Siemens P3	Syntex $P2_1$
a/Å	14.201(2)	10.080(2)
b/Å	9.971(1)	
c/Å	9.493(1)	9.114(2)
β/deg	130.371(8)	
V/Å^3	1024.1(3)	926.0(3)
Z	4	4
F(000)	392	376
μ/cm^{-1}	0.91	1.00
d/g cm^{-3}	1.156	1.249
$2\theta_{max}$/deg	90	75
Number of measured reflections	8470	4090
R_{int}	0.0295	0.0536
Number of independent reflections	3311	1787
R_1 calculated using reflections with $I > 2\sigma(I)$	0.0396 (based on 2505 reflections)	0.0361 (based on 1164 reflections)
wR_2	0.1162 (based on 3311 reflections)	0.0991 (based on 1787 reflections)
GOF	1.031	0.834

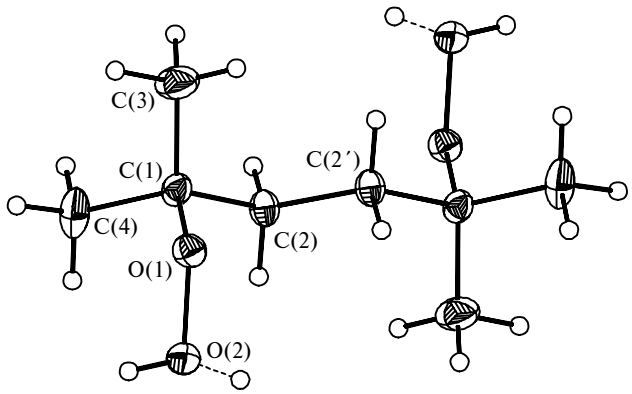

Fig. 1. Overall view of molecule **1**. The non-hydrogen atoms are represented as probability ellipsoids (p = 50%) of thermal vibrations. The second position of the H atom is shown by dashed line.

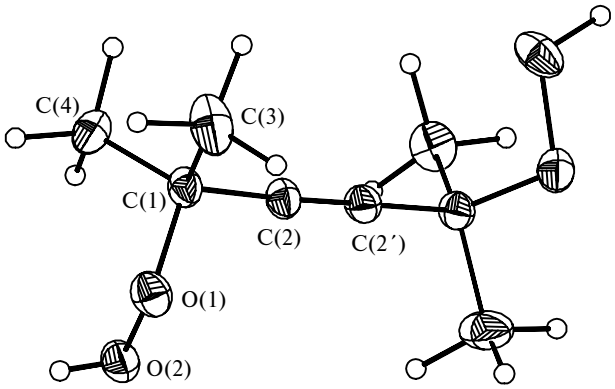

Fig. 2. Overall view of molecule **2**. The non-hydrogen atoms are represented as probability ellipsoids (p = 50%) of thermal vibrations.

Table 5. Principal bond lengths (d) and bond angles (ω) in molecules **1** and **2** based on the X-ray diffraction data and those in the model compounds **1A** and **2A** based on the results of DFT calculations (B3LYP/6-311++G(d,p))

Parameter	**1**	**2**	**1A***	**2A***
Bond		d/Å		
O(1)—O(2)	1.470(1)	1.449(1)	1.459	1.446
O(1)—C(1)	1.454(1)	1.454(1)	1.453	1.452
C(2)—C(2A)**	1.526(1)	1.204(2)	1.529	1.202
C(1)—C(2)	1.534(1)	1.526(2)	1.531	1.473
C(1)—C(3)	1.526(1)	1.523(1)	1.504	1.535
C(1)—C(4)	1.524(1)	1.468(1)	1.531	1.533
Bond angle		ω/deg		
C(1)—O(1)—O(2)	108.45(4)	107.70(7)	109.44	109.91
O(1)—C(1)—C(4)	110.73(4)	110.05(8)	109.87	110.65
O(1)—C(1)—C(3)	101.25(4)	102.32(9)	101.48	101.35
O(1)—C(1)—C(2)	110.48(4)	110.83(8)	109.43	109.61

* The atomic numbering schemes for the molecules **1A** and **2A** are identical with those used for the molecules **1** and **2** (see Figs. 1 and 2, respectively).

** The atom was generated from the basis atom by the symmetry transformation $(-x + 1/2, -y + 1/2, -z + 2)$ for **1** and $(-y + 1, -x + 1, z + 1/2)$ for **2**.

molecules results in some lengthening of the bond. For instance, the O—O bond length in sterically strained structures MeOOH, MeOOMe, and $Bu^t_2O_2$ changes from 1.443 to 1.478 Å (see Refs. 30 and 35). On the contrary, this bond in the F_2O_2 molecule is abnormally shortened to 1.200 Å.[36] A similar trend is also observed for the structures of **1** and **2** (see Table 5). In particular, replacement of the dimethylene bridge by acetylene one leads to shortening of the O(1)—O(2) bond from 1.470(1) to 1.449(1) Å, whereas the lengths of the hydrogen bonds in crystals **1** and **2** remain unchanged.

Both molecules are characterized by nearly equal parameters of torsional motion (twisting about the O—O bond), *viz.*, the torsion angle H—O—O—C is −111.3 and 118.4° in **1** (for two positions of the H atom) and 113.9° in **2**. These values are close to one another, which is typical of hydroperoxides[37] and indicates that substituents have little effect on the conformation of the hydroperoxide group.

A distinguishing feature of the molecular geometry of **1** and **2** is a decrease in the bond angle O(1)—C(1)—C(3) as compared to the tetrahedral angle down to 101.25(4)° and 102.32(9)°, respectively. Similar distortions of the bond angles in the oxygen-containing (broadly, heteroatom-containing) tetrahedral sites with C_3 symmetry were reported in the literature.[32] They are called the d-effect.[35]

Our analysis of the O—C—C bond angle distribution in the Bu^t—O fragment (a total of 640 structures)* showed that in all structures one O—C—C angle is much smaller than the rest three angles (100—104° *vs.* 107—110°, respectively). The distribution of the O—C—C bond angles in the Bu^tO fragment is bimodal with clearly defined maxima at 102° and 110°, the latter being twice as high as the former. It should be emphasized that the decrease in the O—C—C bond angles is observed only for those C atoms which occupy antiperiplanar positions with respect to the substituent at the O atom and cannot be involved in the n-σ*-interaction with the LEP of the O (X) atom. In particular, structures **1** and **2** are characterized by the X—O(1)—C(1)—C(3) torsion angles of ~60°, whereas the X—O(1)—C(1)—C(4) and X—O(1)—C(1)—C(4) angles are close to 180°.

Similar distortions of the O—C—C angles occur not only in the crystalline state. Our B3LYP/6-311++G(d,p) quantum-chemical calculations of model hydroperoxides Me_2EtC—O—OH (**1A**) and $(HC{\equiv}C)Me_2C$—O—OH (**2A**), which can be considered related to the experimentally studied compounds, showed that structure peculiarities observed in the crystals are also retained in the isolated molecules (see Table 5). We found that this computational method allows a rather correct reproduction of the experimental geometric parameters, except for the O—O distance in molecule **1A**. As in the crystal, replacement of the Et group by the acetylide fragment in molecules **1A** and **2A** leads to substantial (by 0.012 Å) shortening of the O—O bond. Both structures **1A** and **2A** are also characterized by distorted O—C—C bond angles for the methyl group (the C(3) atom), which is in the synclinal position with respect to the LEP of the O(1) atom.

Electron density distribution in the crystals of 1 and 2

Analysis of the electron density distribution in the crystals of **1** and **2** was carried out using the multipole refinement and the XD program package[39] in the framework of the Hansen—Coppens model.[38]

Similarly to the previously studied compounds containing the O—O bond,[4,6] the static DED maps constructed for molecules **1** and **2** show that the character of the electron density distribution in the region of this bond is essentially different from the character of all other covalent bonds. The cross-sections of the DED in the OOH plane in hydroperoxides **1** and **2** (Fig. 3) demonstrate that, in contrast to homopolar C—C bonds (Fig. 4, *a*), accumulation of the DED in this plane is observed only in the regions of the LEP of O atoms and in the regions of the O—H bonds, whereas the regions of the O—O bond in both hydroperoxides is characterized by a depletion of the electron density (the so-called negative DED).

If the last-named result obtained for molecules **1** and **2** is consistent with our expectation, the results of the topological analysis of $\rho(\mathbf{r})$ in the crystals are to be clarified taking into account ambiguity of the determination of the character of interatomic O—O interaction from the results of quantum-chemical calculations (see Table 3).

* Analysis was performed for ordered organic structures with $R < 0.1$.

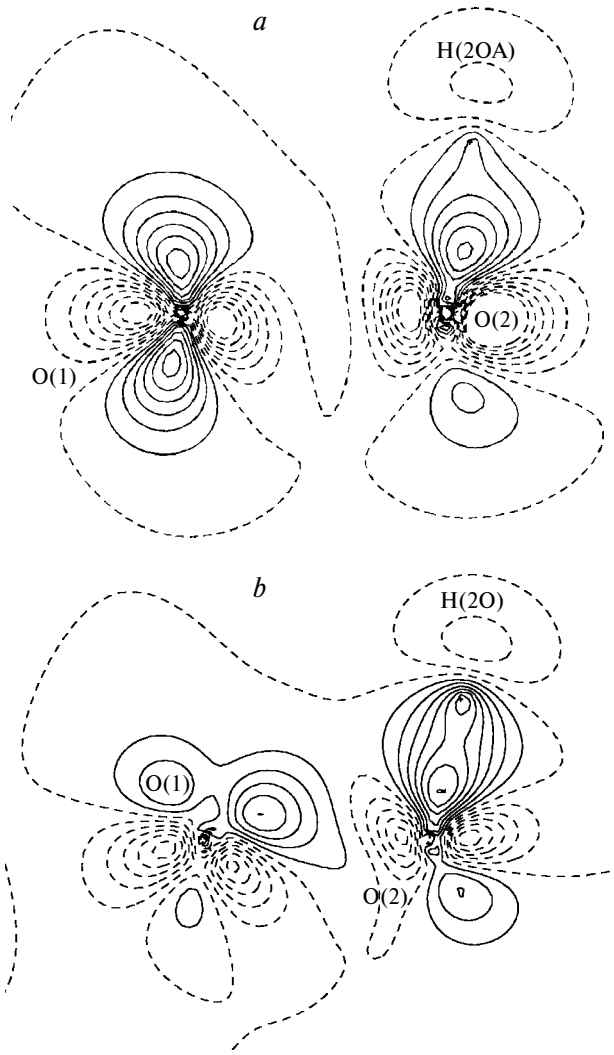

Fig. 3. Cross-sections of the static deformation electron density in the crystals of hydroperoxides **1** (*a*) and **2** (*b*) in the plane passing through the O, O, and H atoms. The maps are contoured at an interval of 0.1 e Å^{-3}. The negative contours are shown as dashed lines.

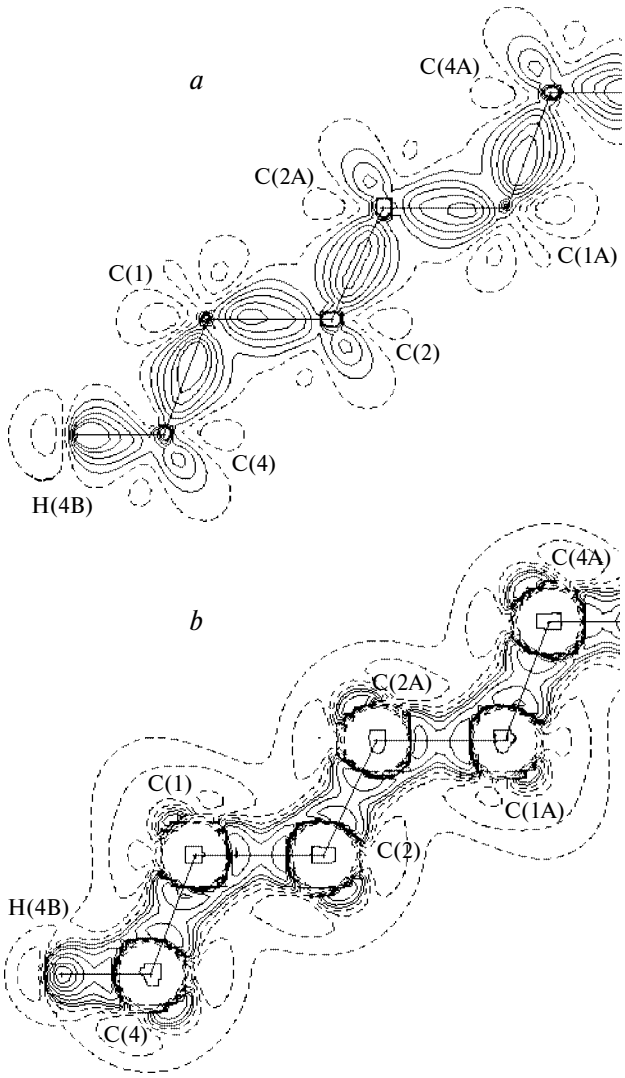

Fig. 4. Cross-sections of the static deformation electron density (*a*) and $-\nabla^2\rho(\mathbf{r})$ (*b*) in the plane passing through the C(4), C(1), and C(2) atoms. The isolines for the DED are drawn with an increment of 0.1 e Å^{-3}, those for $-\nabla^2\rho(\mathbf{r})$ are given in the logarithmic scale. The negative contours are shown as dashed lines.

Analysis of the cross-sections of the Laplacian $-\nabla^2\rho(\mathbf{r})$* in the plane passing through the O—O bonds in hydroperoxides **1** and **2** (Fig. 5) shows that, similarly to the corresponding DED maps, the regions of the O—O bonds in the interatomic space are characterized by positive values of $-\nabla^2\rho(\mathbf{r})$. This corresponds to depletion of $\rho(\mathbf{r})$ and is typical of both closed-shell interactions and intermediate type of interactions. On the contrary, accumulation of $\rho(\mathbf{r})$ is observed near the LEP of the O atoms and in the regions of the O—H, O—C, and C—C bonds (see Fig. 4, *b* and Fig. 5). Therefore, the electron density distributions for the homopolar bonds C—C and O—O in the crystals of **1** and **2** differ not only in the DED maps, but also in the $-\nabla^2\rho(\mathbf{r})$ maps irrespective of the choice of the reference state.

Analysis of the CT of the $\rho(\mathbf{r})$ in molecules **1** and **2** showed that the CT (3, −1) are located not only in the regions of the C—C, O—C, and O—O bonds, but also in the regions of intermolecular hydrogen bonds O—H...O. The principal topological characteristics of the electron density distribution at the CT (3, −1) in the crystals of **1** and **2** are listed in Table 6. For comparison, we also performed the topological analysis of $\rho(\mathbf{r})$ in the molecules of model compounds **1A** and **2A** using the results of DFT (B3LYP/6-311++G(d,p)) calculations.

As can be seen from the data listed in Table 6, all bonds in molecules **1** and **2**, except for the O—O and

* To put the regions of the electron density accumulation in the DED and $\nabla^2\rho(\mathbf{r})$ maps into correspondence with each other, the function $-\nabla^2\rho(\mathbf{r})$ is presented in the cross-sections.

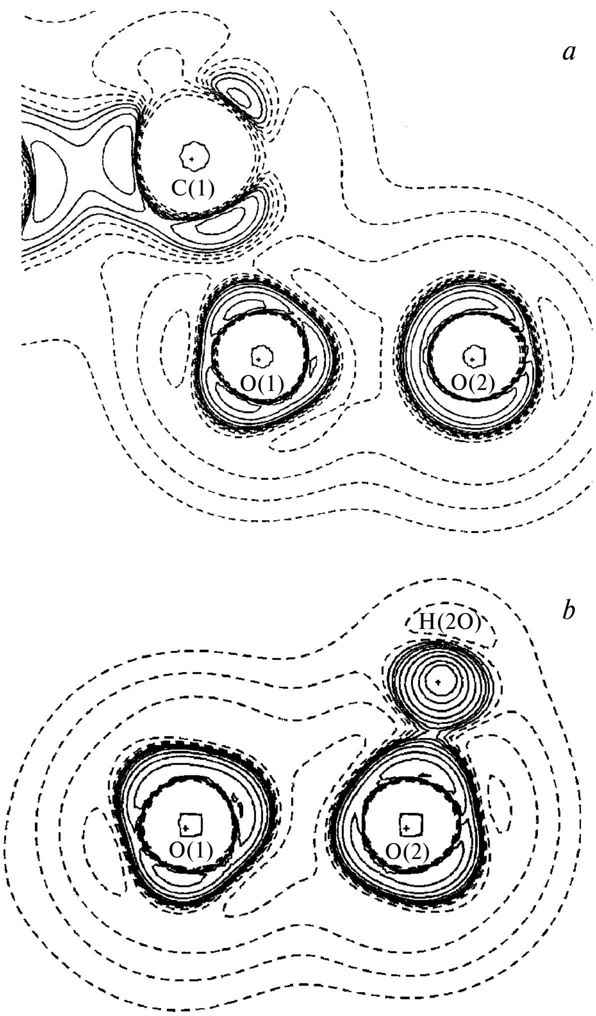

Fig. 5. Cross-sections of $-\nabla^2\rho(\mathbf{r})$ in the plane passing through the O(1), O(2), and C(1) atoms in the crystal of **1** (*a*) and in the plane passing through the O(1), O(2), and H(20) atoms in the crystal of **2** (*b*). The isolines are drawn in the logarithmic scale. The negative contours are shown as dashed lines.

intermolecular H-bonds, are characterized by negative $\nabla^2\rho(\mathbf{r})$ values and, hence, correspond to covalent interactions. On the contrary, the O—O and O—H...O bonds are characterized by positive $\nabla^2\rho(\mathbf{r})$ values and, hence, can belong either to the intermediate type of interactions or to closed-shell interactions. However, the topological characteristics $\rho(\mathbf{r})$ of these bonds are substantially different. In particular, the $\nabla^2\rho(\mathbf{r})$ and $\rho(\mathbf{r})$ values for the H-bonds are an order of magnitude lower than for the O—O bonds (see Table 6). The $|\lambda_1/\lambda_3|$ ratios for the O—O bonds in **1** and **2** are also much larger than for the H-bonds. On the other hand, they are close to the $|\lambda_1/\lambda_3|$ ratio at the CT (3, −1) in the region of the F—F bond. In contrast to nearly zero theoretical value of the Laplacian for the H_2O_2 molecule, large positive values of $\nabla^2\rho(\mathbf{r})$ for crystals **1** and **2** at the CT (3, −1) in the region of the O—O bond (18.75 and 17.73 e Å^{-5}, respectively) should be emphasized. This allows unambiguous assignment of the O—O interaction in molecules **1** and **2** to the intermediate type.

Comparison of the topological characteristics of the electron density distributions in hydroperoxides **1** and **2** and in model compounds **1A** and **2A** reveals retention of qualitative features of the chemical bonding on going from the crystal to the gas phase (see Table 6). For instance, in the gas phase all bonds, except for the O—O bond, are characterized by negative values of the Laplacian at the CT (3, −1), whereas $\nabla^2\rho(\mathbf{r}) > 0$ in the region of the O—O bonds in both molecules. However, the absolute values of $\nabla^2\rho(\mathbf{r})$, especially for the C—O and O—O bonds, are substantially different (see Table 6). Such differences between the $\nabla^2\rho(\mathbf{r})$ values for isolated molecules and crystals were reported in the literature.[40–42] They are usually explained by an increase in the bond polarity caused by the effect of the crystal field.[40] For instance, the value of $\nabla^2\rho(\mathbf{r})$ at the CT (3, −1) in the region of the N—O bond obtained from calculations[42] for an isolated molecule and a crystal of *p*-nitroaniline changed from −35.1 to −12.4 e Å^{-5}

Table 6. Principal topological characteristics of the electron density distribution at the CT (3, −1) in the crystals of **1** and **2** based on the X-ray diffraction data and in molecules **1A** and **2A** based on the results of B3LYP/6-311++G(d,p) calculations

Bond	**1**			**2**			**1A**			**2A**		
	$\rho(\mathbf{r})$ /e Å^{-3}	$\nabla^2\rho(\mathbf{r})$ /e Å^{-5}	$\|\lambda_1/\lambda_3\|$	$\rho(\mathbf{r})$ /e Å^{-3}	$\nabla^2\rho(\mathbf{r})$ /e Å^{-5}	$\|\lambda_1/\lambda_3\|$	$\rho(\mathbf{r})$ /e Å^{-3}	$\nabla^2\rho(\mathbf{r})$ /e Å^{-5}	$\|\lambda_1/\lambda_3\|$	$\rho(\mathbf{r})$ /e Å^{-3}	$\nabla^2\rho(\mathbf{r})$ /e Å^{-5}	$\|\lambda_1/\lambda_3\|$
O(1)—O(2)	1.99	18.75	0.30	1.79	17.73	0.31	1.82	1.67	0.48	1.87	1.03	0.48
O(1)—C(1)	1.70	−7.42	0.75	1.52	−1.49	0.71	1.61	−10.77	1.05	1.79	−12.34	1.10
C(1)—C(2)	1.59	−9.49	0.99	1.65	−6.40	1.08	1.66	−13.66	1.29	1.64	−16.59	1.52
C(1)—C(3)	1.67	−11.10	1.05	1.45	−3.72	1.03	1.65	−13.63	1.29	1.62	−13.20	1.28
C(1)—C(4)	1.71	−12.05	1.11	1.47	−4.55	1.02	1.66	−13.66	1.29	1.61	−13.19	1.28
C(2)—C(2A)*	1.63	−9.64	1.01	2.54	−20.44	2.10	1.61	−11.86	1.60	2.70	−28.92	6.11
O(2)—H(2OA)	1.89	−23.24	1.10	2.19	−26.78	1.3	2.48	−61.45	1.76	2.46	−61.12	1.75
O(2)—H(2OB)	1.99	−26.13	1.15									
H(2OA)...O(2′)	0.17	4.00	0.14	0.17	4.34	0.12						
H(2OB)...O(2″)	0.22	3.89	0.12									

* The atom was generated from the basis atom by the symmetry transformation (−*x* + 1/2, −*y* + 1/2, −*z* + 2) for **1** and (−*y* + 1, −*x* + 1, *z* + 1/2) for **2**.

(*cf.* −10.6 e Å^{-5} obtained based on the results of X-ray diffraction study of *p*-nitroaniline).

Thus, the results of our quantum-chemical and X-ray diffraction studies of the nature of interatomic interactions F—F (in the F_2 molecule) and O—O (in the hydroperoxides containing both electron-donor and electron-acceptor substituents at the atoms) show that the homopolar bonds F—F and O—O are essentially different from conventional covalent bonds. On the one hand, they are characterized by depletion of the electron density in the interatomic space, which is typical of ionic and highly polar bonds. On the other hand, a distinguishing feature of these bonds is domination of the local density of the potential energy, which is typical of covalent bonding. Our conclusion that the interatomic interactions O—O and F—F belong to the intermediate type is consistent with the results of a recent theoretical study of the H_2O_2 and F_2 molecules by the valence bond method[43] and with those of the topological analysis of the electron localization function (ELF) in 1,2,7,8-tetraaza-4,5,10,11-tetraoxatricyclo[6.4.1.1^{2,7}]tetradecane.[44]

Experimental

The principal crystallographic data and refinement parameters for the structures of **1** and **2** are listed in Table 4. The structures were solved by direct methods and refined by the full-matrix least-squares method in the anisotropic-isotropic approximation based on F^2. Position of the hydrogen atoms were located from the difference electron density maps and all were included in the final refinement with isotropic thermal parameters. All calculations were carried out on a personal computer using the SHELXTL PLUS program package (Version 5.0).

For all non-hydrogen atoms in molecules **1** and **2**, the coordinates, anisotropic thermal parameters, and the multipole parameters up to the octupole level ($l = 3$) were refined without symmetry restrictions, except for the C(2) atom of molecule **2**, for which the spherical harmonics satisfying cylindrical symmetry were also refined. Positions of the hydrogen atoms and their isotropic thermal parameters were not refined. Before the refinement, the C—H and O—H distances were normalized to the "ideal" neutron diffraction values of 1.07 and 0.988 Å, respectively. The H atoms were refined up to the dipole level ($l = 1$) with consideration of cylindrical symmetry. Correctness of the anisotropic parameters of atomic displacements was evaluated using Hirshfeld's test, [45] which was found to be at most $7 \cdot 10^{-4}$ Å^2 for the C—C and O—C bonds. The multipole refinement converged to $R = 0.022$, $wR = 0.024$, GOF = 1.35, and $N_{ref}/N_{par} = 8.63$ for the structure of **1** and to $R = 0.028$, $wR = 0.0214$, GOF = 0.98, and $N_{ref}/N_{par} = 7.44$ for the structure of **2**. The electron density maxima in the residual electron density maps ($\rho(\mathbf{r})_{exp} - \rho(\mathbf{r})_{multip}$) for the crystals of **1** and **2** were no higher than 0.13 e Å^{-3}.

The authors express their gratitude to N. L. Allinger (University of Georgia, Athens, USA) for help in performing quantum-chemical calculations and to A. Yu. Kosnikov and V. L. Antonovskii (N. N. Semenov Institute of Chemical Physics, Russian Academy of Sciences) for providing the samples.

This work was carried out with the financial support of the Russian Foundation for Basic Research (Project Nos. 00-15-97359, 00-03-32807a, 99-07-90133).

References

1. P. Coppens, *Angew. Chem., Int. Ed. Engl.*, 1977, **16**, 32.
2. D. Feil, *Chemica Scr.*, 1986, **26**, 395.
3. V. G. Tsirel´son and M. Yu. Antipin, in *Problemy kristallokhimii* [*Problems of Crystal Chemistry*], Ed. M. A. Porai-Koshits, Nauka, Moscow, 1989, 116 (in Russian).
4. J.-M. Savariault and M. S. Lehmann, *J. Am. Chem. Soc.*, 1980, **102**, 1298.
5. M. Yu. Antipin and Yu. T. Struchkov, *Metalloorg. Khim.*, 1989, **2**, 128 [*Organomet. Chem. USSR*, 1989, **2** (Engl. Transl.)].
6. J. D. Dunitz and P. Seiler, *J. Am. Chem. Soc.*, 1983, **105**, 7056.
7. R. F. W. Bader, W. H. Henneker, and P. E. Cade, *J. Chem. Phys.*, 1967, **46**, 3341.
8. D. Lauvergnat and P. C. Hiberty, *J. Mol. Struct. (THEOCHEM)*, 1995, **338**, 283.
9. E. A. Robinson, S. A. Johnson, T.-H. Tang and R. J. Gillespie, *Inorg. Chem.*, 1997, **36**, 3022.
10. K. S. Pitzer, *J. Am. Chem. Soc.*, 1947, **70**, 2140.
11. R. S. Mulliken, *J. Am. Chem. Soc.*, 1950, **72**, 4493.
12. R. T. Sanderson, *Polar Covalence*, Academic Press, New York, 1983.
13. K. L Kunze and M. B. Hall, *J. Am. Chem. Soc.*, 1986, **108**, 5122.
14. K. L Kunze and M. B. Hall, *J. Am. Chem. Soc.*, 1987, **109**, 7611.
15. W. H. E. Schwarz, L. Menshing, P. Valtazanos, and W. Von Niessen, *Int. J. Quant. Chem.*, 1986, **29**, 909.
16. W. H. E. Schwarz, P. Valtazanos, and K. Ruedenberg, *Theor. Chim. Acta*, 1985, **68**, 471.
17. R. F. W. Bader, *Atoms in Molecules. A Quantum Theory*, Clarendron Press, Oxford, 1990.
18. D. Cremer and E. Kraka, *Croat. Chim. Acta*, 1984, **57**, 1259.
19. R. F. W. Bader and H. Essen, *J. Chem. Phys.*, 1984, **80**, 1943.
20. R. F. W. Bader, *J. Chem. Phys. A*, 1998, **102**, 7314.
21. Yu. Abramov, *Acta Crystallogr.*, 1997, **A53**, 264.
22. R. Bianchi, G. Gervasio, and D. Marabello, *Inorg. Chem.*, 2000, **39**, 2360.
23. S.-G. Wang and W. H. E. Schwarz, *Angew. Chem., Int. Ed.*, 2000, **39**, 1757.
24. V. G. Tsirelson and R. P Ozerov, *Electron Density and Bonding in Crystals: Principles, Theory, and X-Ray Diffraction Experiments in Solid State Physics and Chemistry*, IOP Publishing Ltd, 1996.
25. V. G. Tsirel´son, *Zh. Fiz. Khim.*, 2000, **74**, 1529 [*Russ. J. Phys. Chem.*, 2000, **74** (Engl. Transl.)].
26. J. Wang, L. A. Eriksson, B. G. Johnson, and R. J. Boyd, *J. Chem. Phys.*, 1996, **100**, 5274.
27. W. J. Hehre, R. Ditchfield, and J. A. Pople, *J. Chem. Phys.*, 1972, **56**, 2257.
28. M. J. Frisch, G. W. Trucks, H. B. Schlegel, P. M. W. Gill, B. G. Johnson, M. A. Robb, J. R. Cheeseman, T. A. Keith, G. A. Petersson, J. A. Montgomery, K. Raghavachari, M. A. Al-Laham, V. G. Zakrzewski, J. V. Ortiz, J. B.

Foresman, J. Cioslowski, B. B. Stefanov, A. Nanayakkara, M. Challacombe, C. Y. Peng, P. Y. Ayala, W. Chen, M. W. Wong, J. L. Andres, E. S. Replogle, R. Gomperts, R. L. Martin, D. J. Fox, J. S. Binkley, D. J. Defrees, J. Baker, J. P. Stewart, M. Head-Gordon, C. Gonzalez, and J. A. Pople, *GAUSSIAN 94*, Pittsburgh (PA), 1995.
29. F. W. Biegler-König, R. F. W. Bader, and T.-H. Tang, *J. Comput. Chem.*, 1982, **3**, 317.
30. D. Christen, H.-G. Mack, and H. Oberhammer, *Tetrahedron*, 1988, **44**, 7363.
31. J. A. Dobado, J. Molina Molina, and D. Portal Olea, *J. Mol. Struc. (THEOCHEM)*, 1998, **433**, 181.
32. J. Koput, *Chem. Phys. Lett.*, 1995, **236**, 516.
33. G. A. Khachkuruzov and I. N. Przheval´skii, *Opt. i Spektr.*, 1974, **36**, 299 [*Opt. Spectrosc. USSR*, 1974, **36** (Engl. Transl.)].
34. J. Koput, *J. Mol. Spectr.*, 1986, **115**, 438.
35. Yu. L. Slovokhotov, T. V. Timofeeva, M. Yu. Antipin, and Yu. T. Struchkov, *J. Mol. Struct.*, 1984, **112**, 127.
36. C. Yamada and E. Hirota, *J. Chem. Phys.*, 1984, **80**, 4694.
37. A. Yu. Kosnikov, V. L. Antonovskii, S. V. Lindeman, Yu. T. Struchkov, I. P. Zyat´kov, and N. A. Turovskii, *Zh. Strukt. Khim.*, 1988, **29**, 125 [*J. Struct. Chem.* (*USSR)*, 1988, **29** (Engl. Transl.)].
38. N. K. Hansen and P. Coppens, *Acta Crystallogr.*, 1978, **A34**, 909.
39. T. T. Koritsansky, S. T. Howard, T. Richter, P. R. Mallinson, Z. Su, and N. K. Hansen, XD, *A Computer Program Package for Multipole Refinement and Analysis of Charge Densities from X-ray Diffraction Data*, 1995.
40. G. Gatti, V. R. Saunders, and C. Roetti, *J. Chem. Phys.*, 1994, **101**, 10686.
41. P. Coppens, Yu. Abramov, M. Carducci, B. Korjov, I. Novozhilova, C. Alhambra, and M. R. Pressprich, *J. Am. Chem. Soc.*, 1999, **121**, 2285.
42. A. Volkov, Yu. Abramov, P. Coppens, and C. Gatti, *Acta Crystallogr.*, 2000, **A56**, 332.
43. S. Shaik, P. Maitre, G. Sini, and P. C. Hiberty, *J. Am. Chem. Soc.*, 1992, **114**, 7861.
44. R. Llusar, A. Beltrán, J. Andérs, S. Noury, and B. Silvi, *J. Comput. Chem.*, 1999, **20**, 1517.
45. F. L. Hirshfeld, *Acta Crystallogr.*, 1976, **A32**, 239.

Received July 20, 2000;
in revised form June 25, 2001